

RESEARCH ARTICLE

Multimomics to investigate the mechanisms contributing to repression of *PTPRC* and *SOCS2* in pediatric T-ALL: Focus on miR-363-3p and promoter methylation

Monika Drobna-Śledzińska¹  | Natalia Maćkowska-Maślak¹  | Roman Jaksik²  |
 Maria Kosmalka¹  | Bronisława Szarzyńska^{1,3}  | Monika Lejman⁴  |
 Łukasz Sędek⁵  | Tomasz Szczepański⁶  | Tom Taghon^{7,8}  |
 Pieter Van Vlierberghe^{8,9}  | Michał Witt¹  | Małgorzata Dawidowska¹ 

¹Institute of Human Genetics Polish Academy of Sciences, Poznań, Poland

²Department of Systems Biology and Engineering, Silesian University of Technology, Gliwice, Poland

³Polish Stem Cells Bank, Warsaw, Poland

⁴Laboratory of Genetic Diagnostics, Medical University of Lublin, Lublin, Poland

⁵Department of Microbiology and Immunology, Zabrze, Medical University of Silesia in Katowice, Zabrze, Poland

⁶Department of Pediatric Hematology and Oncology, Medical University of Silesia in Katowice, Zabrze, Poland

⁷Department of Diagnostic Sciences, Ghent University, Ghent, Belgium

⁸Cancer Research Institute Ghent, Ghent, Belgium

⁹Department of Biomolecular Medicine, Ghent University, Ghent, Belgium

Correspondence

Monika-Drobna-Śledzińska and Małgorzata Dawidowska, Institute of Human Genetics, Polish Academy of Sciences, Strzeszyńska 32, 60-479 Poznań, Poland.

Email: monika.drobna@igcz.poznan.pl and malgorzata.dawidowska@igcz.poznan.pl

Funding information

European Commission; Narodowe Centrum Badań i Rozwoju; Narodowe Centrum Nauki; European Union's Horizon 2020 research and innovation program, Grant/Award Number: 952304; National Centre of Research and Development, Grant/Award Number: STRATEGMED3/304586/5/NCBR/2017; National Science Centre, Grant/Award Numbers: 2018/02/X/NZ2/01833, 2017/25/N/NZ2/01132, 2014/15/B/NZ2/03394, 2021/41/N/NZ2/02247

Abstract

T-cell acute lymphoblastic leukemia (T-ALL) is a heterogeneous and aggressive malignancy arising from T-cell precursors. MiRNAs are implicated in negative regulation of gene expression and when aberrantly expressed contribute to various cancer types, including T-ALL. Previously we demonstrated the oncogenic potential of miR-363-3p overexpression in a subgroup of T-ALL patients. Here, using combined proteomic and transcriptomic approaches, we show that miR-363-3p enhances cell growth of T-ALL in vitro via inhibition of *PTPRC* and *SOCS2*, which are implicated in repression of the JAK-STAT pathway. We propose that overexpression of miR-363-3p is a novel mechanism potentially contributing to overactivation of JAK-STAT pathway. Additionally, by combining the transcriptomic and methylation data of T-ALL patients, we show that promoter methylation may also contribute to downregulation of *SOCS2* expression and thus potentially to JAK-STAT activation. In conclusion, we highlight aberrant miRNA expression and aberrant promoter methylation as mechanisms, alternative to mutations of JAK-STAT-related genes, which might lead to the upregulation of JAK-dependent signaling in T-ALL.

This is an open access article under the terms of the [Creative Commons Attribution-NonCommercial-NoDerivs](https://creativecommons.org/licenses/by-nc-nd/4.0/) License, which permits use and distribution in any medium, provided the original work is properly cited, the use is non-commercial and no modifications or adaptations are made.

© 2022 The Authors. *Genes, Chromosomes and Cancer* published by Wiley Periodicals LLC.

KEYWORDS

acute lymphoblastic leukemia, JAK-STAT pathway in cancer, noncoding RNAs in cancer, oncogenic miRNAs, silencing tumor suppressor genes, T-ALL

1 | INTRODUCTION

T-cell acute lymphoblastic leukemia (T-ALL) is an aggressive hematological malignancy, characterized by high genetic and epigenetic heterogeneity. Several T-ALL subtypes can be identified based on the expression of oncogenic transcription factors and the activation of specific signaling pathways driving disease development and progression.^{1,2} Thus, development of novel therapeutic strategies targeting these pathways is an attractive option for treatment improvements. However, the identification of patients eligible for targeted therapies based solely on the detection of genetic aberrations in genes implicated in these pathways may not be sufficient. It will not reveal these T-ALL cases, in which the activation of a particular pathway is caused by aberrant gene expression, due to deregulation of miRNAs or methylation of CpG islands within gene promoters. Both miRNAs and DNA methylation may act as oncogenic mechanisms, as an alternative to mutations affecting genes encoding components of a given signaling pathway.

Previously we have demonstrated the oncogenic properties of miRNAs encoded in the mir-106a-363 cluster, including miR-363-3p, which is overexpressed in pediatric T-ALL samples compared to normal T-cells.^{3,4} We showed its anti-apoptotic and pro-proliferative effects in T-ALL cell lines and that these effects are mediated by the repression of *PTEN* and *BIM* tumor suppressors.⁴ However, the oncogenic potential of a given miRNA in cancer usually results from the net effect of its action toward multiple target genes. Here, we aim at unraveling the global transcriptomic and proteomic effect of miR-363-3p expression in T-ALL *in vitro*. We demonstrate, for the first time, that overexpression of this miRNA in T-ALL leads to downregulation of the *PTPRC* and *SOCS2* genes, the negative regulators of JAK-STAT signaling, thus potentially contributes to activation of this pathway. We also show that other pathways downstream from JAK might be affected by upregulation of miR-363-3p. JAK-STAT is a ligand-dependent signal transduction pathway involved in the regulation of immune response, cell division, and cell death. Upregulation of this pathway has been shown to contribute to the progression of many cancers, including leukemias.^{5,6} Genetic aberrations leading to constitutive activation of this pathway have been identified in almost 30% of T-ALL cases: mutations in *JAK3*, interleukin-7 receptor (*IL7R*) and *JAK1* being the most frequent.^{7,8} We postulate that upregulation of miR-363-3p may act as a complementary or alternative mechanism contributing to overactivation of this pathway. Additionally, we identified a negative correlation between *SOCS2* expression and its promoter methylation in a subgroup of T-ALL patients. In conclusion, we propose aberrant miRNA expression affecting *PTPRC* and *SOCS2* and aberrant *SOCS2* promoter methylation as mechanisms potentially contributing to upregulation of JAK-dependent signaling in T-ALL.

2 | MATERIALS AND METHODS

2.1 | Patient and control samples

Bone marrow samples were obtained from 54 patients with pediatric T-ALL at the time of diagnosis. Samples were collected at the centers of Polish Pediatric Leukemia and Lymphoma Study Group, with informed consent of the patients/legal guards, in accordance with the Declaration of Helsinki. The study was approved by the Ethics Committee of the Medical University of Silesia (KNW/0022/KB1/145/I/11/12). The clinical characteristics of the T-ALL patients are shown in Table S1. Thymocyte CD4⁺ CD8⁺ and CD34⁺ samples, obtained from children undergoing cardiac surgery (UZ Gent), were used as controls. Immature CD34⁺ thymocytes were purified based on MACS purification using CD34 microbeads (Miltenyi Biotec) without lineage depletion, while CD4 and CD8 labeling was used to sort the CD4⁺ CD8⁺ double-positive subset by a FACSAriaIII (BDBiosciences). The purity of each subset was at least 98%. Human thymus samples were used following the guidelines of, and were approved by, the Ethical Committee of the Ghent University Hospital (Belgium).

2.2 | Cell lines and cell culture

The HEK293T cell line was a kind gift from Prof. Maciej Kurpisz (Institute of Human Genetics, Polish Academy of Sciences). Cells were cultured under standard conditions in Dulbecco's modified Eagle's medium (Gibco, Thermo Fisher Scientific) with 10% fetal bovine serum (FBS; Gibco, Thermo Fisher Scientific), and 1% penicillin/streptomycin solution (Sigma Aldrich). The DND-41 T-cell acute lymphoblastic leukemia cell line was purchased from the Leibniz Institute DSMZ—German Collection of Microorganisms and Cell Cultures. The ALL-SIL T-cell acute lymphoblastic leukemia cell line was a kind gift from Prof. Pieter Van Vlierberghe (Cancer Research Institute Ghent, CRIG). Cells were cultured under standard conditions in RPMI-1640 medium (Gibco, Thermo Fisher Scientific) with 10% or 20% of FBS (Gibco, Thermo Fisher Scientific) for DND-41 and ALL-SIL, respectively.

2.3 | Expression vectors and oligonucleotide design

For miR-363-3p inhibition, shRNA coding sequences were purchased in form of DNA oligonucleotides from Genomed and cloned into a miRZip pGreenPuro knockdown vector (System Biosciences). As a control for shRNA experiments, a miRZip pGreenPuro scrambled

vector was used (System Biosciences). pGreenPuro scrambled control and empty backbone vectors were a kind gift from Prof. Anke van den Berg and Dr. Joost Kluiver (University Medical Center Groningen).⁹

For the Dual-Luciferase Reporter Assay, 3'UTR sequences of the *PTPRC* and *SOCS2* genes were amplified using primers listed in Table S2 and cloned into pmirGLO vector (Promega). Additionally, sequences coding a putative miRNA response element (MRE) for hsa-miR-363-3p in *PTPRC* and *SOCS2* 3'UTRs, flanked by 30 nt on each side, were cloned into the pmirGLO vector. For rescue experiments, four-point mutations were introduced to the MRE region during the oligonucleotide synthesis step to abolish the miRNA-mRNA interaction.

For miR-363-3p overexpression, the pre-miRNA sequence was amplified and cloned into the pCDH-CMV-MCS-EF1-GreenPuro overexpression vector (System Biosciences).

For lentiviral particles assembly, the pRSV.REV, pMSCV-VSV-G, and pMDLg/PRRE vectors (Addgene) were used. These vectors were a kind gift from Agnieszka Dzikiewicz-Krawczyk (Institute of Human Genetics, Polish Academy of Sciences).

All sequences of primers and oligonucleotides are listed in Table S2.

2.4 | Lentiviral transduction

For assembly of lentiviral particles, HEK293T cells were seeded on six-well culture plate. Upon 70%–80% confluence, the cells were transfected with 600 ng of each: pRSV.REV, pMSCV-VSV-G, and pMDLg/PRRE packing vectors and 1200 ng of transfer vector. Transfection was performed using the JetPrime DNA/siRNA Transfection Kit (Polyplus Transfection). After 24 h, the transfection medium was replaced with 1 ml fresh medium. After 48 h, the medium was collected and filtered with 0.45 µm filters. For transduction of DND-41, cells were seeded on 12-well plate in 400 µl of RPMI-1640 medium. Then, 400 µl of filtered medium, containing lentiviral particles, was added to each well. Additionally, 200 µl of TransDux Max Enhancer (System Biosciences) and 2 µl TransDux Reagent (System Biosciences) was added. For transduction of ALL-SIL, cells were seeded on six-well plate in 1.8 ml of RPMI-1640 medium, after which 200 µl of filtered medium containing lentiviral particles was added to each well. Polibrene Reagent (Sigma Aldrich) was added to each well at the final concentration of 8 µg/ml. Cells were spinfected for 90 min (at 1500 rpm and 32°C). Antibiotic selection of transduced cells was started 3–4 days post-transduction. For selection, puromycin dihydrochloride (Gibco, Thermo Fisher Scientific) was used at the concentration of 10 µg/ml. The selection procedure was conducted for 14 days. The effectiveness of transduction was assessed with the use of CytoFlex S flow cytometer (Beckman Coulter) with GFP as a marker.

2.5 | GFP competition assay

DND-41 and ALL-SIL cell lines were transduced with miRZip scrambled control vector or miRZip miR-363-3p vector with the efficiency

30%–50% without puromycin selection. Cells were cultured on a six-well plate. Three days post-transduction, half of the cells from each well were harvested and the percentage of transduced (GFP⁺) cells was assessed using CytoFlex S flow cytometer (Beckman Coulter). Cells were harvested every 3 days for 18 days and the percentage of GFP⁺ cells for each well was calculated as a fold change of the percentage of GFP⁺ cells in the first tested time point. The experiment was performed in three independent biological replicates.

2.6 | Quantitative proteomic analysis

For proteomic analysis, 10⁶ transduced DND-41 cells were lysed in 200 µl buffer containing 1% sodium dodecyl sulfate (SDS) and 30 µM Tris-HCl (pH 8). The cells were incubated in 95°C for 5 min with shaking. The amount of protein in cell lysates was quantified with the BCA Protein Assay Kit (Pierce, Thermo Fisher Scientific). The preparation of protein samples for TMT labeling and quantitative analysis and mass spectrometry procedure was conducted by the Mass Spectrometry Laboratory at the Institute of Biochemistry and Biophysics of Polish Academy of Sciences. The experiment was performed in five independent biological replicates.

The protein samples were purified and digested using Filter Aided Sample Preparation procedure. The digestion was carried out overnight using trypsin/LysC mix (Promega) in 1:25 enzyme-to-protein ratio at 37°C. The peptides were labeled with Tandem Mass Tag (TMT) 10plex Set (Thermo Fisher Scientific) and the labeling efficiency was checked before combining the samples. TMT labeled samples were subjected to high-pH reverse-phase fractionation. Separation was performed using the Waters Acquity UPLC H-class system. The peptide elution was monitored at 214 nm by UV detector. Twenty-five fractions from each TMT set were dried in Speedvac and reconstituted in 100 µl 0.1% trifluoroacetic acid (TFA) and 2% ACN prior to LC-MS/MS analysis. Fractions were analyzed using the LC-MS system composed of the ACQUITY UPLC M-Class System (Waters) directly coupled to a QExactive mass spectrometer (Thermo Fisher Scientific).

Offline recalibration, as well as peptides and proteins identification, was performed in the MaxQuant/Andromeda software suite (version 1.6.2.3) using *Homo sapiens* protein sequences derived from Swissprot database (version 2020_04: 563082 total entries). The search included tryptic and LysC-generated peptides, Methylthio (C) set as a fixed modification and Oxidation (M) as a variable one. Reporter MS2 quantification was specified to obtain values for quantitative analysis. Reverse database was used for target/decoy statistical results validation, peptide, and protein FDR was set to 0.01.

Protein groups along with quantitative data were further analyzed in Perseus (version 1.6.2.3). Data were cleaned (hits from reversed database and contaminants were removed) and log₂ was transformed for better data distribution. TMT reporter values were normalized with Internal Reference Scaling (IRS) using reference channels to take into account that data were distributed in two separate TMT experiments. Missing values were replaced with data from normal

distribution (width 0.3, down shift 1.8) separately for each column. Subsequently, two-sample *t*-test with permutation-based FDR was performed to compare expression changes between groups. Significance threshold for resulting *q*-value was 0.05.

2.7 | RNA extraction and RT-qPCR

The miRNeasy RNA Isolation Kit (Qiagen) was used for the extraction of total RNA including the recovery of the small RNA fraction. RNA isolates were DNase treated and purified with the use of the RNA Clean and Concentrator Kit (Zymo Research). RNA concentration was measured with Quantus Fluorometer (Promega) using Qubit HS RNA Assay Kit (Thermo Fisher Scientific). RNA integrity was determined with the 4200 TapeStation using High Sensitivity RNA ScreenTape (Agilent Technologies). For miRNA quantification, total RNA was reverse transcribed with TaqMan Advanced miRNA cDNA Synthesis Kit (Thermo Fisher Scientific) according to the manufacturer's protocol. TaqMan Fast Advanced Master Mix and predesigned TaqMan Advanced miRNA assays (Thermo Fisher Scientific) were used. Three endogenous control miRNAs (hsa-miR-16-5p, hsa-let-7a-5p, and hsa-miR-25-3p) were selected using a strategy based on a comprehensive assessment of expression stability in our miRNA-seq data and in RT-qPCR, as previously described.¹⁰ RT-qPCR analyses were conducted in two technical and three biological replicates with the use of the 7900HT Fast Real-Time PCR System (Applied Biosystems). The comparative deltaCT method ($\Delta\Delta\text{CT}$) and Data Assist Software v.3.01 (Thermo Fisher Scientific) were used for relative quantification of expression.¹¹

2.8 | RNA sequencing and bioinformatics analysis

Library preparation and next-generation sequencing were performed by NGS Service Macrogen. For sequencing of the T-ALL patient samples, libraries were constructed from 1 μg of total RNA, using the TruSeq Stranded mRNA library protocol based on poly(A) enrichment, according to the manufacturer's instruction (TruSeq Stranded mRNA Sample Preparation Guide, Part #15031047 Rev. E; Illumina). We introduced a modification to the protocol—reduced fragmentation time (90°C for 2 min), as previously described.¹² For sequencing of RNA obtained from transduced DND-41 cell line, libraries were generated with the TruSeq Stranded mRNA Kit (Illumina) with a standard protocol. The quality of all the libraries was assessed based on size distribution and concentration using the TapeStation D1000 Screen Tape (Agilent Technologies). Libraries were sequenced on the Illumina NovaSeq6000 platform, using the following settings; for T-ALL patient samples: 2x150PE (paired-end sequencing with 150 nt reads), read depth of coverage: 150 million reads/sample; for DND-41 cell line: 2x150PE, 60 million reads/sample.

Pre-alignment quality control was conducted using FastQC¹³ and FastQ Screen.¹⁴ Sequencing adapters were removed using Trim Galore¹⁵ and reads shorter than 20 nt after trimming were discarded.

Adapter trimmed reads were aligned to the GRCh38 reference genome using STAR ver. 2.7.3a,¹⁶ with NCBI Reference Sequence transcript database (GCF_000001405.39_GRCh38.p13) as suggested in Zhao et al.¹⁷ Read counts for individual genes were obtained using featureCounts from the Subread package.¹⁸ Post-alignment quality control statistics were extracted from STAR reports, samtools (stats),¹⁹ RSeQC,²⁰ and Picard.²¹ Differentially expressed genes (DEGs) were identified using edgeR,²² with Bonferroni multiple testing correction.

2.9 | Overrepresentation analysis

Differentially expressed genes (DEGs) were tested for overrepresentation among biological processes and pathways, represented by relevant terms in Kyoto Encyclopedia of Genes and Genomes (KEGG), Reactome, Hallmarks of Cancer, and Gene Ontology (GO). Overrepresentation of pathway-associated genes among those differentially expressed upon miR-363-3p inhibition was tested using Fisher's exact test for pathways originating from the KEGG, Reactome, and Hallmarks of Cancer databases. GO processes were selected using conditional hypergeometric test implemented in the Bioconductor GOSTats package (ver. 2.46). In all cases, Benjamini and Hochberg's multiple testing correction was applied with a significance threshold of 0.05. The magnitude of overrepresentation was assessed based on odds ratio (OR) values, calculated using the following formula:

$$OR = \frac{q/k}{m/t}$$

where *q* is the number of DEGs involved in a given biological process, *k* is the total number of DEGs, *m* is the number of genes in a given process/pathway, and *t* is the total number of genes reported in a given database.

2.10 | Identification of miRNA binding sites

For the identification of putative target genes for miR-363-3p among the list of genes encoding proteins upregulated upon miR-363-3p inhibition, we used a Pearl script designed to search for miRNA binding sites in 3'UTRs, based on the RefSeq transcripts, as described previously.⁹ The advantage of this analysis over the standard miR target prediction tools is the possibility to identify all types of canonical miR binding sites (6mer, 7mer-A1, 7mer-m8, and 8mer), including also the weak 6mer sites.

2.11 | Dual-luciferase reporter assay

Selected predicted miRNA–mRNA interactions were validated with the Dual-Glo Luciferase Reporter Assay (Promega) as described previously.⁴ Briefly, HEK 293 T cells were seeded on 24-well culture plate

24 h before transfection. Cells were subjected to transfection at 60%–80% confluency using the JetPrime DNA/siRNA Transfection Kit (Polyplus Transfection) to enable co-transfection with miR-363-3p coding or empty pCDH-CMV-MCS-EF1-GreenPuro vector (System Biosciences) and pmirGLO plasmids (Promega), containing 3'UTRs of the selected target genes. About 250 and 50 ng of pCDH and pmirGLO plasmid, respectively, were added per well. Luciferase activity was measured with GloMax-Multi+ Detection System (Promega) after 72 h from transfection. All experiments were performed in four replicates. A significant decrease in luciferase activity relative to control (negative control miRNA) was indicative of direct interaction between the seed sequence of the miRNA (defined as the nucleotides at positions 2–7 of the 5' end of mature miRNA sequences) and the MRE in the 3'UTR of target mRNA.

2.12 | Western blot

About 10^7 cells were lysed in 100 μ l of RIPA buffer with a protease inhibitor cocktail and EDTA (Thermo Fisher Scientific). Protein concentration was determined using Pierce BCA Protein Assay Kit (Thermo Fisher Scientific). Proteins were separated on 4%–15% Mini-PROTEAN TGX Stain-free Gel (Bio-Rad). After electrophoresis, proteins were transferred onto a 0.45- μ m PVDF Low Fluorescence membrane (Bio-Rad). Membranes were blocked using 5% non-fat milk and incubated with 1:2000 anti-CD45 antibody (610266, BD Biosciences), 1:2000 anti-SOCS2 antibody (#2779, Cell Signaling Technology), or 1:10000 anti- β -tubulin antibody (ab131205, Abcam). After washing, membranes were incubated with horseradish peroxidase (HRP) conjugated with 1:10,000 anti-mouse secondary antibody (A9917, Sigma Aldrich) or 1:40,000 anti-rabbit secondary antibody (ab97051, Abcam). Immunoreactive protein bands were detected with Clarity Western ECL Substrate for HRP (Bio-Rad) on Chemidoc Imaging System (Bio-Rad). The abundance of target protein was assessed in reference to β -tubulin loading control using Image Lab 6.0.1 software (Bio-Rad). Each experiment was conducted in three biological replicates.

2.13 | Integrative gene expression and promoter methylation analysis

Methylation levels (beta values) obtained using Illumina Infinium HumanMethylation450 BeadChips²³ were compared to the normalized read counts obtained using RNA-seq based on Illumina TruSeq stranded mRNA protocol (deposited in ArrayExpress under the accession number E-MTAB-11759), for a common cohort of 48 T-ALL patients, for whom both mRNA-seq and methylation data were available. For each gene, we conducted a test for association between paired samples, using Spearman's rho, based on normalized read counts from RNA-seq and beta values obtained using methylation probes that fall within the promoter region (defined as +5000 and –500 bp from the transcription start site). Signals obtained from multiple probes per single promoter region were averaged. Correction for

multiple testing was carried out using the Benjamini–Hochberg method.

2.14 | Statistical analysis

For the comparison of two independent means, data were analyzed for normality with the Shapiro–Wilk test and next the two groups were tested for equality of variances. Statistical significance of the results was calculated with the unpaired t-test or nonparametric Mann–Whitney test. For GFP competition assay, statistical significance was calculated with two-way ANOVA test. These analyses and data visualization were performed with the GraphPad Prism 8 software.

Association between relapse occurrence and patient clusters identified based on *JAK–STAT* gene expression levels was evaluated using the Pearson's χ^2 test, by the use of *ggstatsplot* R library (v.0.9.1). Additional association between the clusters and patient survival was evaluated using survival curves prepared with the *survminer* R library (v.0.4.9).

3 | RESULTS

3.1 | miR-363-3p inhibition contributes to loss of growth advantage of T-ALL cells in vitro

To investigate the role of miR-363-3p, overexpressed in T-ALL patients, we selected two T-ALL cell lines with high endogenous level of this miRNA, DND-41, and ALL-SIL^{3,24} and performed stable repression of this miRNA using the miRZip miRNA inhibition system. We showed, using the green fluorescence protein (GFP) growth competition assay, that inhibition of miR-363-3p resulted in loss of growth advantage of both tested T-ALL cell lines. This was reflected by the decreased percentage of GFP positive cells (transduced with miRZip miR-363-3p vector) as compared to control cells (transduced with a scrambled vector) upon 18 days of culture (Figure 1), observed in both cell lines. Thus, we confirmed the oncogenic properties of miR-363-3p in T-ALL in vitro.

3.2 | Global transcriptomic and proteomic effects of miR-363-3p inhibition in T-ALL in vitro

To investigate the global effects of miR-363-3p on gene expression, we applied a combined transcriptomic and proteomic approach in a T-ALL cell line upon stable inhibition of miR-363-3p. We performed mRNA sequencing and mass spectrometry-based quantitative proteomic analysis in DND-41 cells transduced with miRZip miR-363-3p vector as compared to DND-41 cells transduced with a scrambled vector as a control. mRNA-seq revealed 127 upregulated and 315 downregulated transcripts upon miR-363-3p inhibition (Table S3). In the proteomic analysis, we found 631 upregulated and

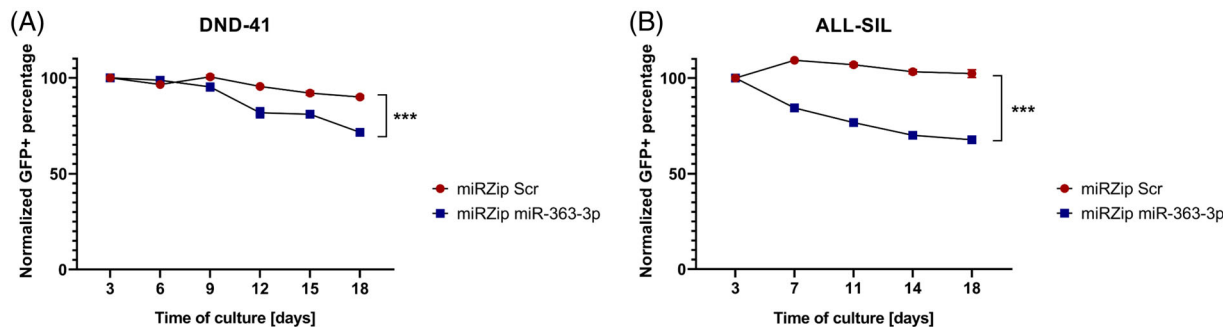


FIGURE 1 Loss of miR-363-3p leads to decreased growth advantage in T-ALL cells with endogenous high expression of this miRNA. GFP growth competition assay upon miR-363-3p inhibition in DND-41 (A) and ALL-SIL (B) T-ALL cell lines upon transduction with miRZip miR-363-3p inhibitor vector or scrambled vector (Scr) as a control. The GFP percentage for each time point was calculated in reference to the GFP percentage at the first day of measurement (Day 3 after transduction). *** $p < 0.001$ (p value calculated by two-way ANOVA for miR-363-3p expression as independent variable).

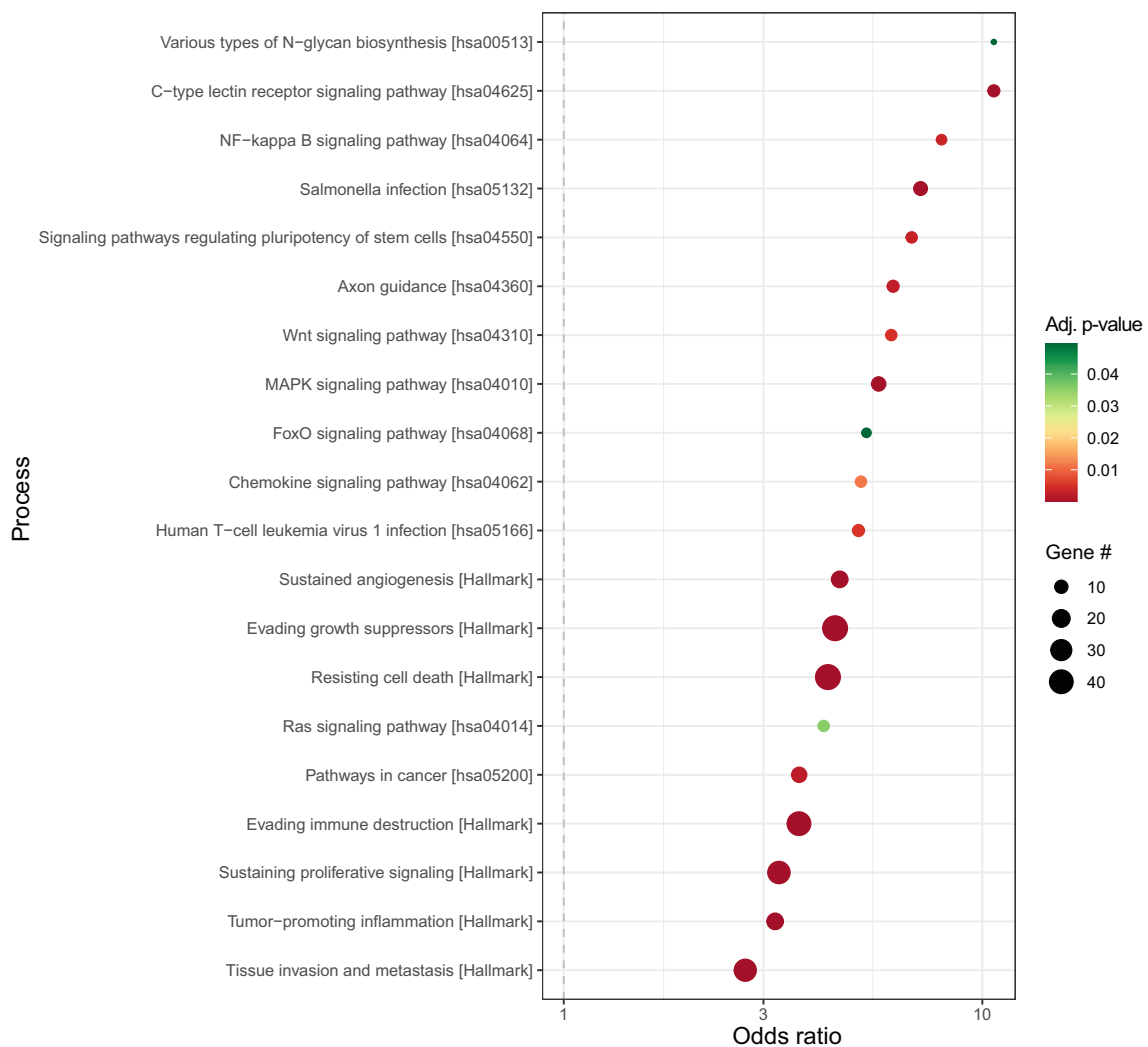


FIGURE 2 Pathway enrichment analysis for mRNAs differentially expressed upon miR-363-3p inhibition as compared to control in DND-41 T-ALL cell line. Odds ratio for the selected pathways and processes, identified using conditional hypergeometric test, with Benjamini and Hochberg correction for multiple testing and 0.05 significance level. The size of the dots (gene count) represents the number of genes involved in each biological process; the color of the dots represents p value. The terms are sorted by odds ratio.

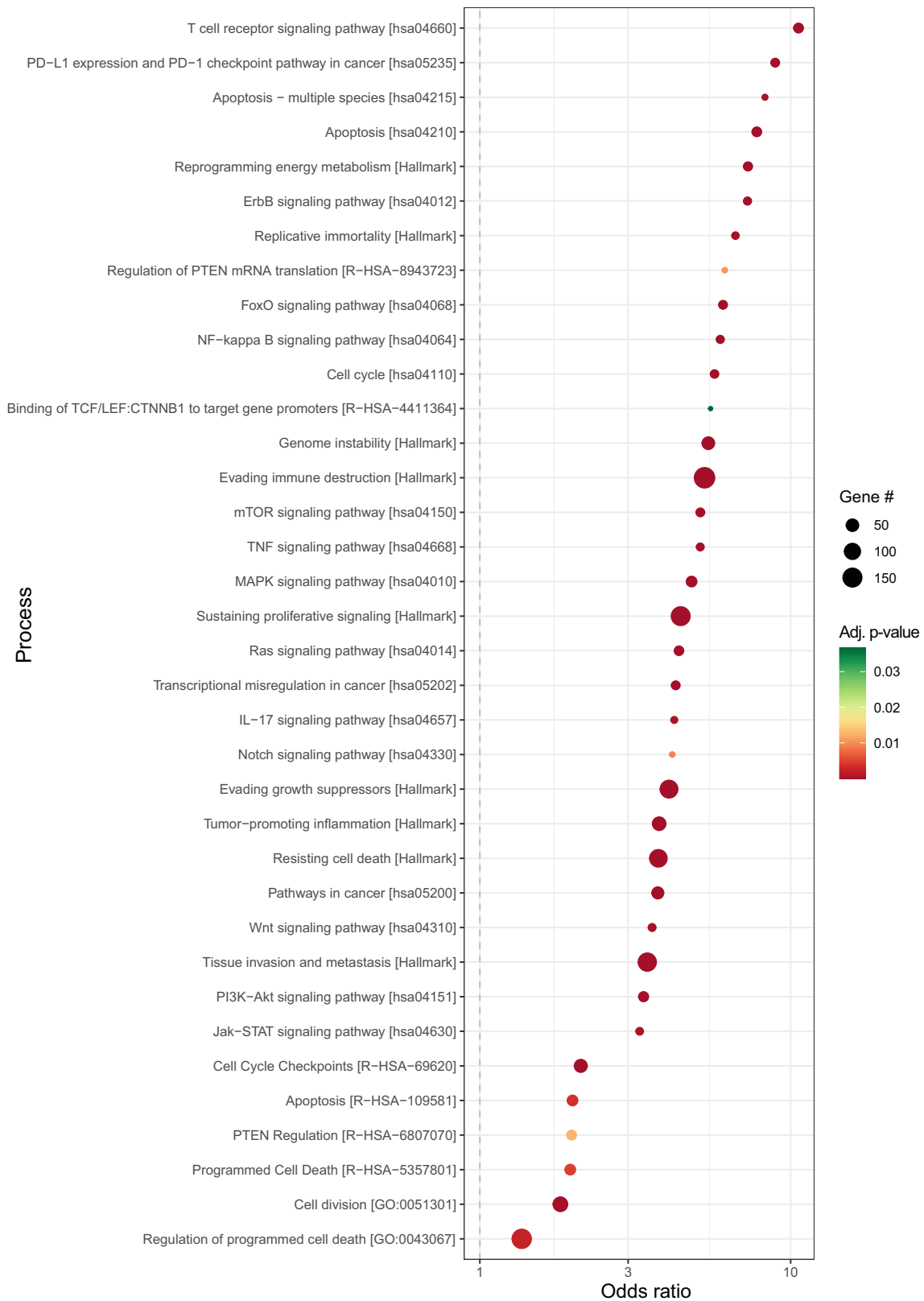


FIGURE 3 Pathway enrichment analysis for genes encoding proteins with differential level upon miR-363-3p inhibition as compared to control in DND-41 T-ALL cell line. Odds ratio for the selected pathways and processes, identified using conditional hypergeometric test, with Benjamini and Hochberg correction for multiple testing and 0.05 significance level. The size of the dots (gene count) represents the number of genes involved in each biological process; the color of the dots represents p value. The terms are sorted by odds ratio.

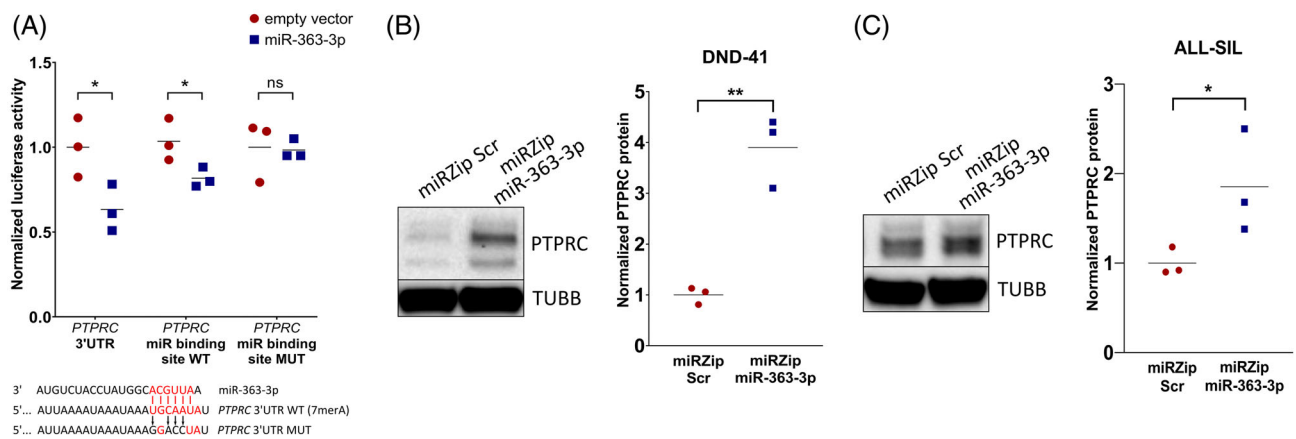


FIGURE 4 miR-363-3p directly inhibits the expression of *PTPRC* in T-ALL cell lines. (A) Dual-Luciferase Reporter Assay for detection of interaction between miR-363-3p and full-length *PTPRC* 3'UTR or 3'UTR fragment containing predicted miRNA binding site (at the positions 828–834 in the 3'UTR flanked by 30 bp on each site). The graphs present the decrease of relative luciferase activity in the presence of miRNA overexpression vector in reference to empty vector. This interaction was diminished upon introducing mutations within the predicted 7mer-A1 miR binding site. Below the graph, the predicted interaction site is shown, with indication of nucleotides mutated in rescue experiment. WT—wild-type sequence; MUT—sequence with mutations introduced within miRNA binding site in 3'UTR; * $p < 0.05$; ns—not significant. (B, C) Western blot evaluation of *PTPRC* protein level in DND-41 (B) and ALL-SIL (C) upon miR-363-3p inhibition (miRZip miR-363-3p) as compared to scrambled control (miRZip Scr) in reference to Tubulin Beta Chain (TUBB) as loading control. The graphs present the mean normalized *PTPRC* protein level from three biological replicates. ** $p < 0.01$.

774 downregulated proteins upon inhibition of this miRNA (Table S4). To investigate cellular functions potentially affected by miR-363-3p, we tested the DEGs and proteins for overrepresentation in biological processes and pathways, defined in GO, KEGG, Hallmarks of Cancer and Reactome databases. We observed a marked overlap between processes revealed by the analysis of transcripts and proteins overrepresentation, with all processes and pathways significantly overrepresented in the transcriptomic analysis (Figure 2, Table S5) and also in the proteomic analysis (Figure 3, Table S6). The importance of these processes for oncogenesis and leukemia biology further supports our hypothesis on the oncogenic role of miR-363-3p in T-ALL. Importantly, the number of differentially expressed proteins (Table S4) and the number of processes revealed by the overrepresentation analysis of genes encoding these proteins (Table S6) were higher than in case of transcripts-based analysis (Table S5). This reflects the fact, that in humans, miRNAs primarily act via suppression of their target transcripts translation and to a lesser extent via transcript degradation.²⁵ Thus, the effects of the negative regulation of gene expression mediated by miRNAs are more often observed as decreased protein levels, than changes in the transcript levels. Hence, to identify targets for which expression is directly regulated by miR-363-3p, we further focused on the results of proteomic analysis.

3.3 | Quantitative proteomic analysis reveals *PTPRC* as a target of miR-363-3p

We performed in silico identification of miR-363-3p binding sites in the 3'UTR of genes encoding proteins, that were significantly upregulated upon miR inhibition and identified 138 genes with at least one

binding site for miR-363-3p (Table S4). To investigate further the potential importance of these genes in T-ALL biology, we examined their expression in T-ALL patients using mRNA-seq data of 54 primary T-ALL samples. We found that 19 of these genes are downregulated in T-ALL samples as compared to controls (Table S4), pointing to their tumor suppressor potential. Among them, we identified *PTPRC*, the negative regulator of an oncogenic JAK–STAT pathway.

We hypothesized that upregulation of miR-363-3p, with consequent downregulation of its target genes, acts as a mechanism (alternative to mutations affecting JAK–STAT signaling) potentially contributing to overactivation of this pathway. We tested whether *PTPRC* is indeed a target of miR-363-3p and demonstrated by Dual-Luciferase Assay a direct interaction between 3'UTR of this gene and this miRNA (Figure 4A). We then tested whether miR-363-3p inhibition affects the expression of *PTPRC*. In DND-41 and ALL-SIL cells (with relatively low expression of *PTPRC* protein as compared to other T-ALL cell lines),²⁶ we showed by Western blot that inhibition of miR-363-3p led to statistically significant increase in *PTPRC* level (Figure 4B,C, Figure S1).

3.4 | Repression of *PTPRC* and *SOCS2* by miR-363-3p might contribute to activation of JAK-dependent pathways in T-ALL

Since *PTPRC* is a negative regulator of JAK kinases, we examined in silico whether other JAK-dependent pathways are affected by the inhibition of miR-363-3p. Again, we searched our lists of pathways and processes revealed by mRNA-seq and proteome analysis upon inhibition of this miRNA. Among the top processes identified by the

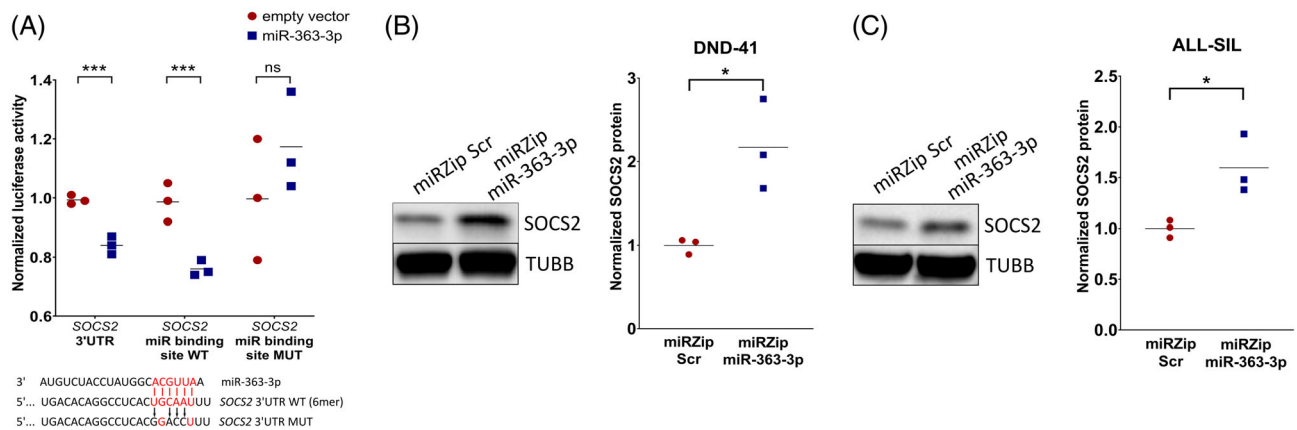


FIGURE 5 miR-363-3p directly inhibits the expression of SOCS2 in T-ALL cell lines. (A) Dual-Luciferase Reporter Assay for detection of interaction between miR-363-3p and full-length SOCS2 3'UTR or 3'UTR fragment containing predicted miRNA binding site (at the positions 413–418 in the 3'UTR flanked by 30 bp on each site). The graphs present the decrease of relative luciferase activity in the presence of miRNA overexpression vector in reference to empty vector. Below the graph, the predicted interaction site is shown, with indication of nucleotides mutated in rescue experiment. WT—wild type sequence; MUT—sequence with mutations introduced within miRNA binding site in 3'UTR; * $p < 0.05$; ns—not significant. (B, C) Western blot evaluation of SOCS2 protein level in DND-41 (B) and ALL-SIL (C) upon miR-363-3p inhibition (miRZip miR-363-3p) as compared to scrambled control (miRZip Scr) in reference to Tubulin Beta Chain (TUBB) as loading control. The graphs present the mean normalized SOCS2 protein level from three biological replicates. * $p < 0.05$; *** $p < 0.001$.

proteomic overrepresentation analysis (Figure 3), we found not only the JAK–STAT pathway but also other oncogenic pathways downstream from JAK–signaling (PI3K/AKT, RAS, mTOR, and FOXO). This observation supports our hypothesis that upregulation of miR-363-3p contributes to the activation of these pathways potentially by the repression of *PTPRC*.

Since many miRNAs tend to be involved in the regulation of multiple genes from the same biological process, we further examined the list of proteins related to JAK-dependent pathways (Table S6) and upregulated upon miR-363-3p inhibition (Table S4). Among them, we identified SOCS2, another negative regulator of the JAK–STAT pathway. This protein is encoded by a gene with three 6mer binding sites for miR-363-3p in its 3'UTR. We confirmed the direct interaction between SOCS2 3'UTR and miR-363-3p via Dual-Luciferase Assay (Figure 5A). By Western blot, we confirmed the increase of SOCS2 protein level in DND-41 and ALL-SIL cell lines upon miR-363-3p inhibition (Figure 5B,C, Figure S2). These results support our hypothesis that upregulation of miR-363-3p leads to repression of two negative regulators of JAK–STAT pathway, the *PTPRC* and SOCS2, and thus might contribute to the activation of JAK-dependent signaling in T-ALL cells.

3.5 | Subgroups of T-ALL patients differ in the expression of JAK–STAT related genes

To investigate further the deregulation of JAK–STAT-related genes in T-ALL primary samples, we used our mRNA-seq data on 46 pediatric T-ALL patients, for which miRNA-seq data are available.³ We performed hierarchical clustering based on the expression of 22 genes directly involved in the regulation of JAK–STAT signaling,

selected based on the literature data. This revealed grouping of patient samples into three main clusters (C1, C2, and C3, according to the main arms of the dendrogram) (Figure 6A). Since there were only two samples in C1 and they largely resemble the expression of C2, we further analyzed these as C1_C2 cluster. Within the C3 cluster, two sub-clusters could be observed (C3A—in the middle and C3B—on the right of the heatmap). The clusters varied mostly in the expression of genes from SOCS family (SOCS2, SOCS1, and SOCS3) and genes encoding interleukin receptors (*IL7R*, *IL6R*, and *IL4R*). Using our previously published miRNA-seq data for the same group of T-ALL patients,³ we analyzed the expression of miR-363-3p in the JAK–STAT related patient clusters. We observed no statistically significant differences in the expression of this miRNA between the clusters (Figure 6B,C) nor did we find an inverse correlation between the expression of this miRNA and *PTPRC* or SOCS2 mRNA (data not shown). This is not surprising, since in humans, miRNAs operate mostly via the inhibition of the translation of their target transcripts rather than their degradation.²⁵ Thus, the effects of miRNA-mediated gene repression might not necessarily be observed as changes in the transcript level and are expected to be observed on the protein level. Interestingly, by comparing the clinical course of the patients from JAK–STAT-related clusters, we observed a clear (although not significant) trend for worse survival probability (Figure 6D,E) and increased risk of relapse (Figure S3) in patients belonging to C3 cluster, especially for C3A cluster. This cluster is characterized by decreased expression of genes from SOCS family (SOCS1–3), being known suppressors of JAK–STAT signaling. This suggests that the worse outcome of patients from this cluster might potentially be in relation to downregulation of the negative regulators of the JAK–STAT pathway. However, further investigation of bigger T-ALL cohorts is necessary to confirm this notion.

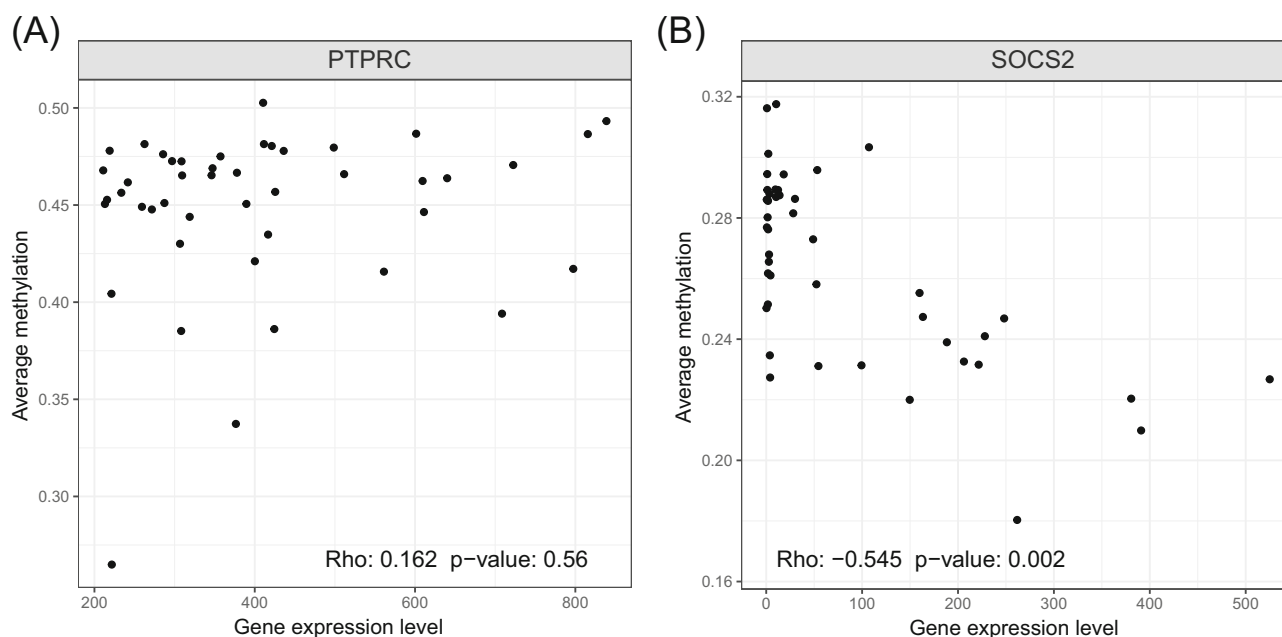


FIGURE 7 The correlation between expression of *PTPRC* (A) and *SOCS2* (B) and methylation of CpG islands in the proximity of their promoter regions in 45 pediatric T-ALL patients calculated with Spearman Rho test with Benjamini–Hochberg correction

3.6 | Repression of *SOCS2* by promoter methylation might contribute to JAK–STAT overactivation in T-ALL

Finally, we investigated if promoter methylation might serve as an additional mechanism of repression of *PTPRC* and *SOCS2*. We tested our mRNA-seq data and EPIC methylation arrays data,²³ obtained in the same cohort of T-ALL patients, for the presence of inverse correlation between the expression of *PTPRC* and *SOCS2* and the methylation of their promoters. For *PTPRC*, we found no significant correlation between promoter methylation and gene expression (Figure 7A). Yet, in case of *SOCS2*, we observed statistically significant inverse correlation (Figure 7B). Although the anticorrelation itself does not directly implicate the mechanism, yet it suggests that the expression of this gene in T-ALL patients is dependent on the methylation status of its promoter. Hence, we conclude that in a subgroup of T-ALL patients, methylation of CpG islands within the promoter of *SOCS2* is a putative mechanism of its downregulation. This might serve as an alternative mechanism to loss-of-function mutations in this gene and may potentially contribute to activation of JAK–STAT pathway.

4 | DISCUSSION

Excessive activation of JAK–STAT pathway and other signaling pathways downstream of JAK signaling is a common phenomenon in T-ALL and in several other malignancies. Frequent upregulation of JAK–STAT signaling in cancers, makes a therapeutic targeting of this

pathway an attractive treatment option.²⁷ Mutations in genes encoding interleukin receptors, JAK kinases, and STAT proteins are considered to be the most prominent factors leading to overactivation of this signaling pathway.^{7,8} Yet, it might also be deregulated due to other mechanisms. Importantly, patients without mutations in component genes of JAK–STAT signaling might potentially also benefit from the treatment regimens aimed to target this pathway. Hence, it is of great importance to unravel all molecular mechanisms that serve as complementation or alternative to genetic aberrations in JAK–STAT-related genes.

The main finding of this multiomic study is the involvement of miR-363-3p in repression of *PTPRC* in T-ALL in vitro. *PTPRC* has been previously reported as a tumor suppressor in T-ALL, implicated in negative regulation of the JAK–STAT pathway. It has been shown in a mouse cytokine-dependent T-ALL cell line (MOHITO) with JAK1 gain-of-function mutation, that inhibition of *PTPRC* contributes to enhanced cell proliferation.²⁶ Although the loss of the *PTPRC* protein was identified in 3.7% of T-ALL pediatric patients and in 12.9% of B-cell precursor ALL (BCP-ALL) patients,²⁸ the loss-of-function mutations in *PTPRC* are very rare and often co-exist with mutations in other JAK–STAT-related genes.²⁶ This suggests that other mechanisms may be implicated in its inactivation. Therefore, we aimed to investigate if miR-363-3p overexpression and promoter methylation affect the expression of genes implicated in JAK-dependent signaling and thus might serve as alternative or additional mechanisms potentially contributing to oncogenic activation of this pathway in T-ALL.

Interestingly, the DND-41 cell line, used in our study, harbors a monoallelic *PTPRC* mutation. Downregulation of *PTPRC* is one of the mechanisms of JAK–STAT activation in this cell line, which is strongly

dependent on the activity of this pathway. Despite the inactivation of one *PTPRC* allele, the *PTPRC* protein is still present in DND-41 cells, although at the much lower level as compared to other T-ALL cell lines.²⁶ On the other hand, the endogenous level of miR-363-3p is relatively high in the DND-41 cell line.^{4,24} Thus, we postulate that overexpression of miR-363-3p acts as an additional or alternative mechanism of *PTPRC* repression in T-ALL cells in vitro and possibly also in a subgroup of T-ALL patients. Our report is the first to present *PTPRC* as a direct target of miR-363-3p in vitro and the first to show that miRNA-mediated regulation results in decreased *PTPRC* expression in T-ALL.

Our second major finding regards *SOCS2*—another negative regulator of the JAK/STAT pathway. *SOCS2* and other proteins belonging to the SOCS family are considered as tumor suppressors.^{29–32} Mutations in SOCS genes are rarely reported in lymphoid malignancies,^{33–35} yet decreased SOCS expression, together with JAK/STAT overactivation, is commonly observed in various cancer types.^{31,36} It suggests the existence of additional mechanisms of its deregulation, alternative to mutations. Thus far, there are only few reports about the regulatory role of miRNAs in the repression of SOCS genes in leukemia and there is no evidence of such regulation in T-ALL.³⁷ The only miRNA described as a negative regulator of *SOCS2* expression in leukemia, is miR-486, reported to be upregulated in acute myeloid leukemia cell lines.³⁸ Here, we present for the first time that the expression of a gene from the SOCS family is regulated by aberrantly expressed miRNAs in T-ALL and we show that *SOCS2* is a direct target of miR-363-3p.

Alongside with the miRNA-mediated repression of *SOCS2*, we show that DNA methylation of the *SOCS2* promoter might act as additional mechanism of inactivation of this putative tumor suppressor in T-ALL. Hypermethylation of CpG islands within promoter regions of tumor suppressor genes is a universal feature of tumorigenesis. Aberrant DNA methylation of *SOCS2* has been reported in 14% of primary ovarian cancers,³⁹ 25% of colorectal cancers⁴⁰ and 43% of melanoma cases.⁴¹ The only study aimed to investigate members of the SOCS gene family in the context of aberrant promoter methylation in T-ALL was that of Sharma et al.⁴² The authors found that DNA methylation causes *SOCS5* silencing and induces activation of JAK–STAT signaling in T-ALL. They showed in vivo that inactivation of *SOCS5* causes leukemic progression in T-ALL xenograft model. Our study is the first to report the significant inverse correlation between *SOCS2* promoter methylation and its expression in T-ALL patients, suggestive of the mechanism of promoter methylation-based repression of *SOCS2*.

In conclusion, by integrating miRNA-seq, mRNA-seq, and methylation data from T-ALL patients and a combined proteomic and transcriptomic approach applied to a T-ALL cell line upon miR-363-3p inhibition, we provide evidence for the oncogenic role of miR-363-3p in T-ALL via repression of *PTPRC* and *SOCS2*, genes implicated in JAK-dependent signaling. We demonstrate that inhibition of miR-363-3p in two T-ALL cell lines contributes to the loss of growth advantage of T-ALL cells in vitro. We additionally indicate the potential role of promoter methylation in the repression of *SOCS2*. We show that in a

subset of T-ALL patients, hypermethylation of promoter CpG islands is inversely correlated with *SOCS2* expression. Thus, we highlight the existence of miRNA-mediated and methylation-based mechanisms potentially contributing to the upregulation of JAK–STAT pathway in T-ALL. The identification of these mechanisms, complementary or alternative to mutations in JAK-related genes, has implications for the development of predictive diagnostics and the identification of patients eligible for treatment options targeting JAK–STAT pathway.

AUTHOR CONTRIBUTIONS

Conceptualization: Monika Drobna-Śledzińska and Małgorzata Dawidowska. *Data curation*: Roman Jaksik. *Formal analysis*: Monika Drobna-Śledzińska, Natalia Maćkowska-Maślak, and Roman Jaksik. *Funding acquisition*: Monika Drobna-Śledzińska, Natalia Maćkowska-Maślak, Małgorzata Dawidowska, Tomasz Szczepański, and Michał Witt. *Investigation*: Monika Drobna-Śledzińska, Natalia Maćkowska-Maślak, Maria Kosmalka, and Małgorzata Dawidowska. *Methodology*: Monika Drobna-Śledzińska, Natalia Maćkowska-Maślak, Maria Kosmalka, and Małgorzata Dawidowska. *Project administration*: Michał Witt and Małgorzata Dawidowska. *Resources*: Monika Lejman (clinical data), Łukasz Sędek, Tom Taghon, Pieter Van Vlierberghe, and Tomasz Szczepański (samples). *Software*: Roman Jaksik. *Supervision*: Małgorzata Dawidowska. *Visualization*: Monika Drobna-Śledzińska, Natalia Maćkowska-Maślak, and Roman Jaksik. *Writing – original draft*: Monika Drobna-Śledzińska, Natalia Maćkowska-Maślak, and Małgorzata Dawidowska. *Writing – review and editing*: Monika Drobna-Śledzińska and Małgorzata Dawidowska. All authors critically revised the manuscript and approved the submitted version.

ACKNOWLEDGMENTS

The authors wish to acknowledge Agnieszka Dzikiewicz-Krawczyk (Institute of Human Genetics Polish Academy of Sciences), Bianka Świdorska and Agata Malinowska (Institute of Biochemistry and Biophysics Polish Academy of Sciences) for precious remarks and discussions. MDŚ and MD were supported by the European Union's Horizon 2020 research and innovation program under Grant agreement no. 952304.

FUNDING INFORMATION

National Science Centre, Poland: 2014/15/B/NZ2/03394; 2017/25/N/NZ2/01132; 2018/02/X/NZ2/01833, 2021/41/N/NZ2/02247; National Centre of Research and Development: STRATEGMED3/304586/5/NCBR/2017. This project has received funding from the European Union's Horizon 2020 research and innovation program under Grant agreement no 952304 (acronym NEXT_LEVEL) within Twinning Action. Calculations were carried out using infrastructure of the Ziemowit computer cluster (www.ziemowit.hpc.polsl.pl) in the Laboratory of Bioinformatics and Computational Biology, The Biotechnology, Bioengineering and Bioinformatics Centre Silesian BIO-FARMA, created in the POIG.02.01.00-00-166/08 and expanded in the POIG.02.03.01-00-040/13 projects.

CONFLICTS OF INTEREST

The authors declare no conflicts of interest.

DATA AVAILABILITY STATEMENT

The data that support the findings of this study are openly available in ArrayExpress at <https://www.ebi.ac.uk/arrayexpress/>, reference number E-MTAB-11366; E-MTAB-11759.

ORCID

Monika Drobna-Śledzińska  <https://orcid.org/0000-0003-1671-9071>

Natalia Maćkowska-Maślak  <https://orcid.org/0000-0002-0296-4597>

Roman Jaksik  <https://orcid.org/0000-0003-1866-6380>

Maria Kosmalka  <https://orcid.org/0000-0002-3951-8013>

Bronisława Szarzyńska  <https://orcid.org/0000-0002-2879-1671>

Monika Lejman  <https://orcid.org/0000-0002-8760-0775>

Łukasz Sędek  <https://orcid.org/0000-0001-9384-914X>

Tomasz Szczepański  <https://orcid.org/0000-0001-5336-261X>

Tom Taghon  <https://orcid.org/0000-0002-5781-0288>

Pieter Van Vlierberghe  <https://orcid.org/0000-0001-9063-7205>

Michał Witt  <https://orcid.org/0000-0003-1729-4159>

Małgorzata Dawidowska  <https://orcid.org/0000-0003-3486-6577>

REFERENCES

- Van Vlierberghe P, Ferrando A. The molecular basis of T cell acute lymphoblastic leukemia. *J Clin Invest*. 2012;122:3398-3406.
- Belver L, Ferrando A. The genetics and mechanisms of T cell acute lymphoblastic leukaemia. *Nat Rev Cancer*. 2016;16:494-507.
- Dawidowska M, Jaksik R, Drobna M, et al. Comprehensive investigation of miRNome identifies novel candidate miRNA-mRNA interactions implicated in T-cell acute lymphoblastic leukemia. *Neoplasia*. 2019;21:294-310.
- Drobna M, Szarzyńska B, Jaksik R, et al. hsa-miR-20b-5p and hsa-miR-363-3p affect expression of PTEN and BIM tumor suppressor genes and modulate survival of T-ALL cells in vitro. *Cells*. 2020;9:1137.
- Brooks AJ, Putoczki T. JAK-STAT signalling pathway in cancer. *Cancers*. 2020;12:1971.
- Vainchenker W, Constantinescu SN. JAK/STAT signaling in hematological malignancies. *Oncogene*. 2013;32:2601-2613.
- Vicente C, Schwab C, Broux M, et al. Targeted sequencing identifies associations between IL7R-JAK mutations and epigenetic modulators in T-cell acute lymphoblastic leukemia. *Haematologica*. 2015;100:1301-1310.
- Liu Y, Easton J, Shao Y, et al. The genomic landscape of pediatric and young adult T-lineage acute lymphoblastic leukemia. *Nat Genet*. 2017;49:1211-1218.
- Niu F, Kazimierska M, Nolte IM, et al. The miR-26b-5p/KPNA2 axis is an important regulator of Burkitt lymphoma cell growth. *Cancers*. 2020;12:E1464.
- Drobna M, Szarzyńska-Zawadzka B, Dąca-Roszak P, et al. Identification of endogenous control miRNAs for RT-qPCR in T-cell acute lymphoblastic leukemia. *Int J Mol Sci*. 2018;19:2858. doi:10.3390/ijms19102858
- Schmittgen TD, Livak KJ. Analyzing real-time PCR data by the comparative C(T) method. *Nat Protoc*. 2008;3:1101-1108.
- Jaksik R, Drobna-Śledzińska M, Dawidowska M. RNA-seq library preparation for comprehensive transcriptome analysis in cancer cells. *Genomics*. 2021;113:4149-4162.
- Babraham Bioinformatics – FastQC A Quality Control Tool for High Throughput Sequence Data. <https://www.bioinformatics.babraham.ac.uk/projects/fastqc/>. Accessed January 17, 2022.
- Wingett SW, Andrews S. Fastq screen: a tool for multi-genome mapping and quality control [version 1; referees: 3 approved, 1 approved with reservations]. *F1000Research*. 2018;7:1338. doi:10.12688/f1000research.15931.1
- Babraham Bioinformatics – Trim Galore!. https://www.bioinformatics.babraham.ac.uk/projects/trim_galore/. Accessed January 18, 2022.
- Dobin A, Davis CA, Schlesinger F, et al. STAR: ultrafast universal RNA-seq aligner. *Bioinformatics*. 2013;29:15-21.
- Zhao S, Zhang B. A comprehensive evaluation of ensembl, RefSeq, and UCSC annotations in the context of RNA-seq read mapping and gene quantification. *BMC Genomics*. 2015;16:95. doi:10.1186/s12864-015-1308-8
- Liao Y, Smyth GK, Shi W. featureCounts: an efficient general purpose program for assigning sequence reads to genomic features. *Bioinformatics*. 2014;30:923-930.
- Li H, Handsaker B, Wysoker A, et al. The sequence alignment/map format and SAMtools. *Bioinformatics*. 2009;25:2078-2079.
- Wang L, Wang S, Li W. RSeQC: quality control of RNA-seq experiments. *Bioinformatics*. 2012;28:2184-2185.
- Picard Tools – By Broad Institute. <https://broadinstitute.github.io/picard/>. Accessed January 17, 2022.
- Robinson MD, McCarthy DJ, Smyth GK. edgeR: a Bioconductor package for differential expression analysis of digital gene expression data. *Bioinformatics*. 2010;26:139-140.
- Roels J, Thénoz M, Szarzyńska B, et al. Aging of preleukemic thymocytes drives CpG Island hypermethylation in T-cell acute lymphoblastic leukemia. *Blood Cancer Discov*. 2020;1:274-289.
- Wallaert A, Van Loocke W, Hernandez L, Taghon T, Speleman F, Van Vlierberghe P. Comprehensive miRNA expression profiling in human T-cell acute lymphoblastic leukemia by small RNA-sequencing. *Sci Rep*. 2017;7:7901.
- Filipowicz W, Bhattacharyya SN, Sonenberg N. Mechanisms of post-transcriptional regulation by microRNAs: are the answers in sight? *Nat Rev Genet*. 2008;9:102-114.
- Porcu M, Kleppe M, Gianfelici V, et al. Mutation of the receptor tyrosine phosphatase PTPRC (CD45) in T-cell acute lymphoblastic leukemia. *Blood*. 2012;119:4476-4479.
- Shouse G, Nikolaenko L. Targeting the JAK/STAT pathway in T cell lymphoproliferative disorders. *Curr Hematol Malign Rep*. 2019;14:570-576.
- Ratei R, Sperling C, Karawajew L, et al. Immunophenotype and clinical characteristics of CD45-negative and CD45-positive childhood acute lymphoblastic leukemia. *Ann Hematol*. 1998;77:107-114.
- Sasi W, Ye L, Jiang WG, Mokbel K, Sharma A. Observations on the effects of suppressor of cytokine signaling 7 (SOCS7) knockdown in breast cancer cells: their in vitro response to insulin like growth factor I (IGF-I). *Clin Transl Oncol*. 2014;16:476-487.
- Chevrier M, Bobbala D, Villalobos-Hernandez A, et al. Expression of SOCS1 and the downstream targets of its putative tumor suppressor functions in prostate cancer. *BMC Cancer*. 2017;17:157.
- Qiu X, Zheng J, Guo X, et al. Reduced expression of SOCS2 and SOCS6 in hepatocellular carcinoma correlates with aggressive tumor progression and poor prognosis. *Mol Cell Biochem*. 2013;378:99-106.
- Das R, Gregory PA, Fernandes RC, et al. MicroRNA-194 promotes prostate cancer metastasis by inhibiting SOCS2. *Cancer Res*. 2017;77:1021-1034.
- Weniger MA, Melzner I, Menz CK, et al. Mutations of the tumor suppressor gene SOCS-1 in classical Hodgkin lymphoma are frequent and associated with nuclear phospho-STAT5 accumulation. *Oncogene*. 2006;25:2679-2684.
- Mottok A, Renné C, Seifert M, et al. Inactivating SOCS1 mutations are caused by aberrant somatic hypermutation and restricted to a subset of B-cell lymphoma entities. *Blood*. 2009;114:4503-4506.

35. Melzner I, Bucur AJ, Brüderlein S, et al. Biallelic mutation of SOCS-1 impairs JAK2 degradation and sustains phospho-JAK2 action in the MedB-1 mediastinal lymphoma line. *Blood*. 2005;105:2535-2542.
36. Chen C-Y, Tsay W, Tang J-L, et al. SOCS1 methylation in patients with newly diagnosed acute myeloid leukemia. *Genes Chromosomes Cancer*. 2003;37:300-305.
37. Keewan E, Matlawska-Wasowska K. The emerging role of suppressors of cytokine signaling (SOCS) in the development and progression of leukemia. *Cancer*. 2021;13:4000.
38. Sha C, Jia G, Jingjing Z, Yapeng H, Zhi L, Guanghui X. miR-486 is involved in the pathogenesis of acute myeloid leukemia by regulating JAK-STAT signaling. *Naunyn Schmiedebergs Arch Pharmacol*. 2021; 394:177-187.
39. Sutherland KD, Lindeman GJ, Choong DYH, et al. Differential hypermethylation of SOCS genes in ovarian and breast carcinomas. *Oncogene*. 2004;23:7726-7733.
40. Letellier E, Schmitz M, Baig K, et al. Identification of SOCS2 and SOCS6 as biomarkers in human colorectal cancer. *Br J Cancer*. 2014; 111:726-735.
41. Liu S, Ren S, Howell P, Fodstad O, Riker AI. Identification of novel epigenetically modified genes in human melanoma via promoter methylation gene profiling. *Pigment Cell Melanoma Res*. 2008;21: 545-558.
42. Sharma ND, Nickl CK, Kang H, et al. Epigenetic silencing of SOCS5 potentiates JAK-STAT signaling and progression of T-cell acute lymphoblastic leukemia. *Cancer Sci*. 2019;110:1931-1946.

SUPPORTING INFORMATION

Additional supporting information can be found online in the Supporting Information section at the end of this article.

How to cite this article: Drobna-Śledzińska M, Maćkowska-Maślak N, Jaksik R, et al. Multiomics to investigate the mechanisms contributing to repression of *PTPRC* and *SOCS2* in pediatric T-ALL: Focus on miR-363-3p and promoter methylation. *Genes Chromosomes Cancer*. 2022; 61(12):720-733. doi:[10.1002/gcc.23085](https://doi.org/10.1002/gcc.23085)